Electronic Interactions in Mixed-Valence and Mixed-Metal Ion Clusters: Inelastic Neutron Scattering Spectra of the Complexes $[Fe^{III}_2M^{II}O(OOCMe)_6(py)_3](py)$, Where M = Mn, Ni

Ross P. White,‡ John A. Stride,† Sarah K. Bollen,† Nittayaporn Chai Sa-Ard,† Gordon J. Kearley,‡ Upali A. Jayasooriya,*,† and Roderick D. Cannon*,†

Contribution from the School of Chemical Sciences, University of East Anglia, Norwich NR4 7TJ, England, and the Institut Laue-Langevin, BP 156X, 38042 Grenoble Cedex, France

Received June 8, 1992

Abstract: Inelastic incoherent neutron scattering spectra are reported for the title complexes. Energy transfers of magnetic origin are observed consistent with transitions between low-lying energy levels of the exchange-coupled metal ion clusters, and excellent agreement is obtained with the Heisenberg spin-only formulation, both as regards the energies and the transition intensities.

Introduction

Trinuclear complexes of the type shown in Figure 1 have assumed considerable importance in the study of electronic interactions between metal ions. They are known with clusters of three identical ions (M^{III}_3O), with various mixed-metal combinations, and with mixed valencies ($M^{III}_2M^{II}O$). Their chemical and physical properties have been reviewed.[1] Two major concerns are the mechanisms of antiferromagnetic coupling and the extent and nature of vibronic interaction in the mixed-valence complexes.[2,3] Our approach to the latter problem has been to compare the properties of the mixed-valence material with those of mixed-metal complexes which differ as little as possible in all respects other than the possibility of electron transfer.[4,5] In a preliminary account of the present work,[6] we compared the inelastic incoherent neutron scattering (IINS) spectra of the series of complexes $[Fe^{III}_2M^{II}O(OOCMe)_6(py)_3](py)$ (**1**, M = Mn, Fe, Co), and we demonstrated significant differences of behavior between the mixed-valence and the mixed-metal systems. In particular, the mixed-valence system showed broader bands and a strong dependence of band shape on temperature.[6] These effects are now beginning to be understood,[3,7,8] and a definitive account will be given in due course. Meanwhile, interesting magnetic anomalies have been discovered in apparently simpler, homonuclear, and homovalent complexes of Cr^{III}_3 and Fe^{III}_3, as reported elsewhere.[9,10] The basis of all our interpretations is the Heisenberg–Dirac–Van Vleck (HDVV) spin-only magnetic coupling scheme. Since we rely on detecting deviations from the predictions of this scheme, we have started here with systems in which the molecular geometry and the ground electronic states of the individual metal ions are as well defined as possible, i.e. the two **1** complexes for M = Mn, Ni. The electronic ground states of the metals involved are orbitally non-degenerate.[11] The iron(III)–manganese(II) complex is known[12–14] to be isomorphous with the iron(III,III,II) compound whose structure has been determined at room temperature.[15] The iron(III)–nickel(II) complex has a different space group,[14] but the molecular structure is evidently similar, as shown by detailed infrared spectroscopic

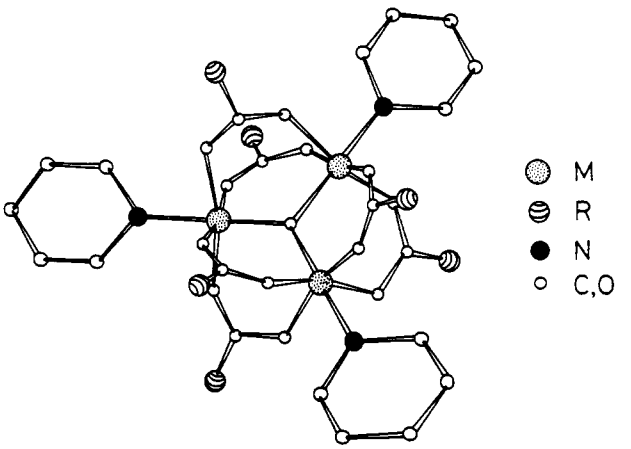

Figure 1. Molecular structure of the complexes $[Fe^{III}_2M^{II}O(OOCMe)_6(py)_3]$, where M = Fe^{III}, M^{II} and R = Me.

† University of East Anglia.
‡ Institut Laue-Langevin.

(1) Cannon, R. D.; White, R. P. *Prog. Inorg. Chem.* **1988**, *36*, 195.
(2) Hendrickson, D. N. Electron transfer in mixed-valence complexes in the solid state. In *Mixed Valency Systems: Applications in Chemistry, Physics and Biology*; Prassides, K., Ed.; NATO ASI Series C: Mathematical and Physical Sciences, Vol 343; Kluwer Academic Publishers: Dordrecht, The Netherlands, 1991; pp 283–298.
(3) Cannon, R. D.; Jayasooriya, U. A.; White, R. P. Inelastic neutron scattering studies of mixed-valency compounds. In *Mixed Valency Systems: Applications in Chemistry, Physics and Biology*; Prassides, K., Ed.; NATO ASI Series C: Mathematical and Physical Sciences, Vol 343; Kluwer Academic Publishers: Dordrecht, The Netherlands, 1991; pp 283–298.
(4) Cannon, R. D.; Montri, L.; Brown, D. B.; Marshall, K. M.; Elliott, C. M. *J. Am. Chem. Soc.* **1984**, *106*, 2591.
(5) Meesuk, L.; Jayasooriya, U. A.; Cannon, R. D. *J. Am. Chem. Soc.* **1987**, *109*, 2009.
(6) White, R. P.; Al-Basseet, J. O.; Cannon, R. D.; Kearley, G. J.; Jayasooriya, U. A. *Phys. B* **1989**, *156–157*, 367.
(7) Cannon, R. D.; Jayasooriya, U. A.; arapKoske, S. K.; White, R. P.; Williams, J. H. *J. Am. Chem. Soc.* **1991**, *113*, 4158.
(8) Jayasooriya, U. A.; Cannon, R. D.; Anson, C. E.; arapKoske, S. A.; White, R. P.; Kearley, G. J. *J. Chem. Soc., Chem. Commun.* **1992**, 379.
(9) Jayasooriya, U. A.; Cannon, R. D.; White, R. P.; Stride, J. A.; Grinter, R.; Kearley, G. J. *J. Chem. Phys.*, in press.
(10) Cannon, R. D.; arapKoske, S. A.; Nielsen, O. V.; Stride, J. A.; Jayasooriya, U. A.; Summerfield, D.; Kearley, G. J.; White, R. P., to be submitted for publication.
(11) Fe(III), Mn(III), high-spin d^5, $t_{2g}^3e_g^2$, $^6A_1$ in a local octahedral or tetragonal field; Ni(II), high-spin d^8, $t_{2g}^6e_g^2$, $^3A_2$. See e.g.: Cotton, F. A.; Wilkinson, G.; Gaus, P. L. *Basic Inorganic Chemistry*, 2nd ed.; John Wiley: New York, 1987; pp 458–9.
(12) Blake, A. B.; Yavari, A.; Kubicki, H. *J. Chem. Soc., Chem. Commun.* **1981**, 796.
(13) Blake, A. B.; Yavari, A. *J. Chem. Soc., Chem. Commun.* **1982**, 1247.
(14) Blake, A. B.; Yavari, A.; Hatfield, W.; Sethulekshmi, C. N. *J. Chem. Soc., Dalton Trans.* **1985**, 2509.
(15) Woehler, R. E.; Wittebort, R. J.; Oh, S. M.; Kambara, T.; Hendrickson, D. N.; Inniss, D.; Strouse, C. E. *J. Am. Chem. Soc.* **1987**, *109*, 1063.

0002-7863/93/1515-7778$04.00/0

studies.[5,16] We find that the spectra of both complexes can be interpreted satisfactorily on the basis of the HDVV model, assuming 2-fold molecular symmetry.

The most general method used so far for studies of magnetic interactions has been the measurement of bulk magnetic susceptibility as a function of temperature. Inelastic incoherent neutron scattering (IINS) is much more informative however since it is a spectroscopic technique, directly observing transitions between individual magnetic states. Furrer and Güdel have pioneered the application of IINS to small metal ion clusters,[17] and Güdel has reviewed the basic theory and the advantages of the method.[18] For present purposes, the main point is that the spin of the neutron enables it to interact with unpaired electrons and thus bring about transitions between magnetic states with appropriate energy transfer, as well as interacting with the atomic nuclei to bring about vibrational transitions. The two types of transitions are distinguished by the different variation of transition probability with momentum transfer (Q). Vibrational transitions increase in intensity with Q^2 whereas magnetic transitions are governed by a magnetic form factor and by interference between the different scattering centers in the cluster, so that at moderate to high Q values they decrease with increasing Q. Güdel *et al.*[17,18] have also shown that for neutron scattering the selection rules are $\Delta S = 0$ or ± 1, for each spin quantum number S of the molecule. Thus in principle it is possible to explore the complete spectrum of magnetic states.

Experimental Section

The complexes were prepared by way of the aquo-adducts $[Fe_2MO(OOCMe)_6(OH_2)_3]\cdot xH_2O$ by methods described previously.[5,12] Satisfactory C, H, and N analyses were obtained, and the pyridine content was determined independently. The complex (0.2 g, accurately weighed) was dissolved in HCl (1 M, 5 mL) and transferred to an all-glass, one-piece steam distillation apparatus.[7,19] To this was added NaOH (1 M, 10 mL) followed by H_2O (20 mL), and the liberated pyridine was steam-distilled into a beaker containing an excess of HCl (1 M, 20 mL). This was titrated against a standard 0.1 M NaOH solution. The first end point corresponds to the neutralization of free acid and the second to the neutralization of pyridinium ion. The difference between the two end points determines the pyridine content, and at the concentrations used this difference could be satisfactorily read from the pH-titration curve. IINS spectra were obtained on the instrument IN4 at the Institut Laue-Langevin, Grenoble, France. Samples, finely powdered, were sealed in aluminium cans, with the thickness calculated to provide *ca.* 10% total scattering. In each case a background spectrum using an empty can was subtracted, and the detectors were calibrated by means of a spectrum of vanadium metal. Data reduction was done with the standard programs PRIME and CROSSX or INX. Scattering angles are defined in the usual way, i.e. 2θ is the angle from vector $\mathbf{k_0}$ to $\mathbf{k_1}$.

Theory: Energies

In the HDVV model,[20] the isotropic spin-coupling Hamiltonian is

$$\mathbf{H_{ex}} = -2\sum J_{ij}\mathbf{S_i}\cdot\mathbf{S_j} \qquad (1)$$

where $\mathbf{S_i}$ and $\mathbf{S_j}$ are the spins on ions i and j. For the present systems we use the coupling scheme $\mathbf{S_a} + \mathbf{S_b} = \mathbf{S_{ab}}$, $\mathbf{S_{ab}} + \mathbf{S_c} = \mathbf{S}$, where subscripts a, b, and c label the two iron(III) atoms and the heteroatom, respectively. The Hamiltonian thus becomes

$$H = -02J(\mathbf{S_a}\cdot\mathbf{S_c} + \mathbf{S_b}\cdot\mathbf{S_c}) - 2J_{ab}(\mathbf{S_a}\cdot\mathbf{S_b}) \qquad (2)$$

and the eigenvalues of energy are

$$E(S,S_{ab}) = -J[S(S+1) - S_{ab}(S_{ab}+1) - S_c(S_c+1)] - J_{ab}[S_{ab}(S_{ab}+1) - 2S_a(S_a+1)] \qquad (3)$$

where S_{ab} takes integer values from 0 to $2S_a$, and S takes values in integer steps from $|S_{ab} - S_c|$ to $(S_{ab} + S_c)$. Plots of $E(S,S_{ab})/J$ against J_{ab}/J thus give families of intersecting straight lines with characteristic patterns for different S_a and S_c. These serve as correlation diagrams for fitting the observed spectra, as shown below.

Intensities

The fundamental equations for incoherent inelastic neutron scattering by magnetic centers are[21]

$$d^2\sigma/d\Omega d\omega = (g\gamma r_0/2)^2 N[Z^{-1}\exp(-E/k_BT)](k_1/k_0)[F(\mathbf{Q})]^2\exp(-2W)\sum_{\alpha,\beta}(\delta_{\alpha,\beta} - Q_\alpha Q_\beta/Q^2)\sum_{i,j}\exp\{i\mathbf{Q}\cdot(\mathbf{R_i} - \mathbf{R_j})\}A^{\alpha\beta}{}_{ij}[\delta(\hbar\omega + E - E')] \qquad (4)$$

$$A^{\alpha\beta}{}_{ij} = \sum_{M,M'}\langle SM|\mathbf{S_i}^{\alpha}|S'M'\rangle\langle S'M'|\mathbf{S_i}^{\beta}|SM\rangle \qquad (5)$$

These refer to scattering by a sample containing N identical centers, undergoing transitions from a state with spin quantum number S, magnetic quantum number M, and energy E to a state with S', M', E', respectively. Z is the partition function, $\hbar\omega$ and $\mathbf{Q}$ are the energy and momentum transferred, $F(\mathbf{Q})$ is the magnetic form factor, $\mathbf{k_0}$ and $\mathbf{k_1}$ are the wavevectors of incoming and scattered neutrons, $\exp(-2W)$ is the Debye–Waller factor, $\mathbf{R_i}$ and $\mathbf{R_j}$ are the position vectors of scattering atoms, and $\mathbf{S}^{\alpha}_i$ is the component of the spin angular momentum operator of atom i, in direction α (α, β = x, y, z). Other symbols have their usual meanings.

Furrer and Güdel,[17] and Hauser,[22] have shown how the model can be extended to coupled systems like the present ones, described by more than one spin quantum number, and they have shown how the tensor-operator method may be applied to evaluate the matrix elements. In particular, they find that $A^{\alpha\beta}{}_{ij} = 0$ unless $\alpha = \beta$, that $A^{\alpha}{}_{ij} = A^{\alpha}{}_{ji}$, and that $A^{x}{}_{ij} = A^{y}{}_{ij} = A^{z}{}_{ij}$. With these substitutions, and with spherical averaging over $\mathbf{Q}$, since our experiments all involve powdered samples, eqs 4 and 5 simplify to

$$\langle d^2\sigma/d\Omega d\omega\rangle = (1/3)K[F(\mathbf{Q})]^2[Z^{-1}\exp(-E/k_BT)]I \qquad (6a)$$

$$I = I_0[\sin(QR)]/QR] \qquad (6b)$$

$$Q^2 = k_0{}^2 + k_1{}^2 - 2k_0k_1\cos 2\theta \qquad (7)$$

where K contains the $\mathbf{Q}$-independent factors, R is the mean metal–metal distance in the cluster, and I_0 is what we shall call the intrinsic scattering probability, given by

$$I_0 = (-1)^{S'+S}[B_{aa} + B_{bb} + B_{cc} + 2(B_{ab} + B_{bc} + 2B_{ca})] \qquad (8)$$

$$B_{ij} = D_iD'_j = \langle S_{ab}S_cS\|\mathbf{T_i}\|S'_{ab}S'_cS'\rangle\langle S'_{ab}S'_cS'\|\mathbf{T_j}\|S_{ab}S_cS\rangle \qquad (9)$$

where $\mathbf{T_i}$ and $\mathbf{T_j}$ are tensor operators. We neglect differences between the form factors of the scattering atoms, since for Fe, Mn, and Ni these are very similar,[23] and we also neglect any

(16) Meesuk, L.; Jayasooriya, U. A.; Cannon, R. D. *Spectrochim. Acta* **1987**, 43A, 687.

(17) (a) Furrer, A.; Güdel, H. U. *J. Phys. C* **1977**, *10*, L91. (b) Güdel, H. U.; Furrer, A. *Mol. Phys.* **1977**, *33*, 1335. (c) Furrer, A.; Güdel, H. U. *Helv. Phys. Acta* **1977**, *50*, 439. (d) Furrer, A.; Güdel, H. U. *Phys. Rev. Lett.* **1977**, *39*, 657. (e) Güdel, H. U.; Stebler, A.; Furrer, A. *Inorg. Chem.* **1979**, *18*, 1091. (f) Güdel, H. U.; Hauser, U.; Furrer, A. *Inorg. Chem.* **1979**, *18*, 2730. (g) Stebler, A.; Furrer, A.; Ammeter, J. H. *Inorg. Chem.* **1984**, *23*, 3496.

(18) Güdel, H. U. In *Magneto-Structural Correlations in Exchange-Coupled Systems*; Willett, R. D., et al., Eds.; D. Reidel: New York, 1975; pp 329–354. Güdel, H. U. In *Understanding molecular properties*; Avery, J., et al., Eds.; D. Reidel: New York, 1987; pp 69–83.

(19) Bodek, I.; Davies, G.; Ferguson, J. H. *Inorg. Chem.* **1975**, *14*, 1708.

(20) Martin, R. L. In *New Pathways in Inorganic Chemistry*; Ebsworth, E. A. V., Maddock, A. G., Sharpe, A. G., Eds.; Cambridge University Press: Cambridge, UK, 1968; pp 175–231.

(21) Marshall, W.; Lovesey, S. W. *The Theory of Thermal Neutron Scattering*; Clarendon Press: Oxford, 1971.

(22) Hauser, U. *Synthese, spektroskopische und magnetochemische Untersuchen an vierkernigen Chrom(III)-komplexen*; Inaugural Dissertation; Universität Bern, 1979.

differences between Fe–Fe and Fe–M bond distances in the Fe_2M triangular clusters.

Noting that $S_a = S_b$ and $S_i = S'_i$, further applications of the Wigner–Eckart theorem lead to

$$D_a = (-1)^{2S_a+S_c+S_{ab}+S'_{ab}+S'+1/2}[(2S+1)(2S'+1)(2S_{ab}+1)(2S'_{ab}+1)S_a(S_a+1)(2S_a+1)]^{1/2}MN \quad (10)$$

and $D'_a = (-1)^{\Delta S}D_a$, $D_b = (-1)^{\Delta S_{ab}}D_a$, $D'_b = (-1)^{\Delta S}D_a$, where $\Delta S = S'-S$ and $\Delta S_{ab} = S'_{ab}-S_{ab}$; and M and N are the following 6-j symbols:[24,25]

$$M = \begin{Bmatrix} S & S' & 1 \\ S'_{ab} & S_{ab} & S_c \end{Bmatrix} \quad (11a)$$

$$N = \begin{Bmatrix} S_{ab} & S'_{ab} & 1 \\ S_a & S_a & S_a \end{Bmatrix} \quad (11b)$$

Similarly

$$D_c = \delta(S_{ab}, S'_{ab})(-1)^{S_c+S_{ab}+S+3/2}[(2S+1)(2S'+1)S_c(S_c+1)(2S_c+1)]^{1/2}L \quad (12)$$

where

$$L = \begin{Bmatrix} S & S' & 1 \\ S_c & S_c & S_{ab} \end{Bmatrix} \quad (13)$$

and $D'_c = (-1)^{\Delta S}D_c$. Expanding the 6-$j$ symbols for the cases $\Delta S_{ab} = 0$, $\Delta S = \pm 1$, we find

$$L = (-1)^{2S_a+S_{ab}+1}2(2S_{ab}+1)\{[2S_a(2S_a+1)(2S_a+2)]/[2S_c(2S_c+1)(2S_c+2)]\}^{1/2}MN \quad (14)$$

Substituting all these results in eqs 8–11 gives finally

$$I_o = 6D_a^2 \quad \text{when } \Delta S_{ab} = 0 \quad (15a)$$

$$I_o = 2D_a^2 \quad \text{when } \Delta S_{ab} = \pm 1 \quad (15b)$$

A general result from these equations is the pair of spin selection rules quoted above, in this case $\Delta S = 0, \pm 1$, and $\Delta S_{ab} = 0, \pm 1$.

Results

$Fe^{III}_2Mn^{II}$ System. A spectrum at $T = 5$ K, obtained with incident neutrons of energy 50 meV (equivalent to 400 cm^{-1}), is shown in Figure 2. Three strong bands are observed, the lowest of which is broad and can be resolved into two bands of similar intensity, here labeled 2a and 2b. Spectra at $T = 50$ K are shown in Figure 3. Band 3 is weakened and a new hot band 6* appears. There is also an apparent increase in intensity of band 2a, which we take to be due to a second hot band 5* overlapping band 2a. The width of the elastic peak in both of these spectra suggests the presence of an unresolved band at ca. 20 cm^{-1}. A spectrum of higher resolution was obtained using neutrons with an incident energy of 28.7 meV (230 cm^{-1}), also at $T = 50$ K (Figure 3). The low-energy band is resolved as shoulder 1, and the combined bands 2a + 5* are separated from band 2b. All these features were confirmed to be of magnetic—i.e. electronic—origin, on the basis of the characteristic angle dependence of intensity implied by eqs 6 and 7. A typical set of spectra at different scattering angles is displayed in Figure 2.

Part of the energy level correlation diagram for the system $S_a = S_c = {}^5/_2$, calculated from eq 3, is shown in Figure 4. The best fit of the number and energies of observed bands was obtained close to $J_{ab}/J = 3.0$. Here there are two low-lying levels, the ground state $|{}^3/_2, 1>$ and first excited state $|5/2, 0>$, and according to the selection rules (15) there is just one state, $|{}^5/_2\ 1>$, which is accessible from both of them. This is consistent with our observation that the broad band 2 contains at least one hot and one cold band, with a separation of the order of 20 cm^{-1}, which is approximately the energy of band 1. On this basis all the allowed transitions match all the observed bands. Assignments are listed in Table I. Energies were refined using a least-squares procedure to give $J = -20.9$ cm^{-1} and $J_{ab} = -61.0$ cm^{-1}.

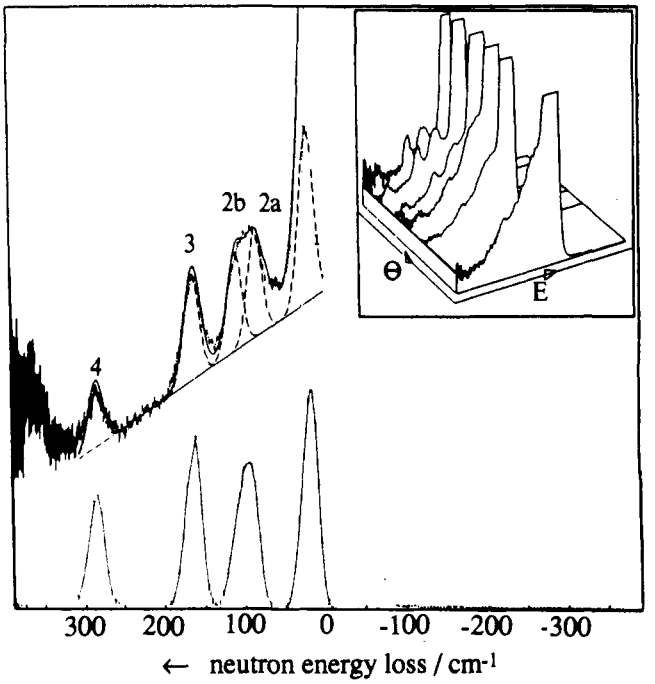

Figure 2. Top left: IINS spectrum (down-scattering) of $[Fe_2MnO(OOCMe)_6(py)_3](py)$ at $T = 5$ K with an incident neutron beam energy of 50 meV. The average scattering angle (2θ) = 12.8°. Original data points are shown with error bars. Broken lines indicate Gaussians fitted to the data with an arbitrary sloping linear baseline; full lines are sums of the calculated bands. Inset: Angular variation of spectra of the same sample. Average scattering angles (2θ), reading from the back, are 4.53, 12.77, 30.40, 46.14, 60.75, 103.19°. Bottom: Calculated spectrum using the parameters listed in Tables I and III.

Relative intensities, calculated from eq 15, are also listed in Table I. Observed band areas are in good agreement with these, as shown by the calculated spectra, at both 5 and 50 K, drawn in Figures 2 and 3. It is significant that the intrinsic intensities (I_o) of the two transitions originating from $|{}^5/_2, 0>$ are two to three times those of the other transitions, and this explains why the hot bands are observed so clearly.

$Fe^{III}_2Ni^{II}$. Spectra over the range 0–480 cm^{-1}, at temperatures of 5–125 K, are shown in Figure 5, and the angular dependences at two temperatures are displayed in Figure 6. In the low-temperature spectrum, strong bands 2 and 3 at 72 and 188 cm^{-1} are clearly magnetic. Weak bands 4 and 5 at 325 and 400 cm^{-1} have phonon character. At higher temperatures another weak band appears at ca. 255 cm^{-1} (Figure 5, band 6*), and this too is possibly magnetic (Figure 6). A spectrum at $T = 5$ K over a lower energy range and at higher resolution shows one more peak (Figure 7, band 1) at ca. 18.5 cm^{-1}. The angular dependence of this peak is less certain, but it is considered to be magnetic.

The correlation diagram for $S_a = {}^5/_2$ and $S_c = 1$, calculated from eq 3, is shown in Figure 8. In principle six ground states are possible, but if we assume $J_{ab}/J \geq 1$ the choice narrows to two, i.e. $|S, S_{ab}> = |0, 1>$ and $|1, 0>$, with the crossover at $J_{ab}/J = 2$. In either case three transitions are allowed, and the ratio of energy differences is the same, that is (band 3 – band 2)/(band 2 – band 1) = 2. This agrees fairly well with the observed ratio (188 – 72)/(72 – 18.5) = 2.17. It is not possible to decide the ground state on the basis of the IINS spectrum, but a value of

(23) Watson, R. E.; Freeman, A. J. *Acta Crystallogr.* **1961**, *14*, 27.
(24) Rotenberg, M.; Bivins, R.; Metropolis, N.; Winston, J. K. *The 3-j and 6-j Symbols*; Technology Press: MIT, Cambridge, MA, 1959.
(25) Edmonds, A. R. *Angular Momentum in Quantum Mechanics*; Princeton University Press: Princeton, NJ, 1960; p 130.

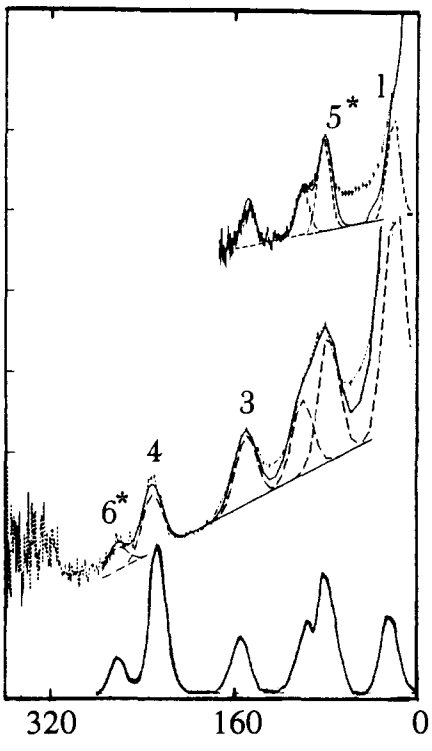

Figure 3. IINS spectra of $[Fe_2MnO(OOCMe)_6(py)_3](py)$. T = 50K. Top: Incident neutron beam energy = 28.67 meV. The average scattering angle (2θ) = 12.8°. Center: Beam energy = 50 meV. Bottom: Calculated spectrum using the parameters listed in Tables I and III.

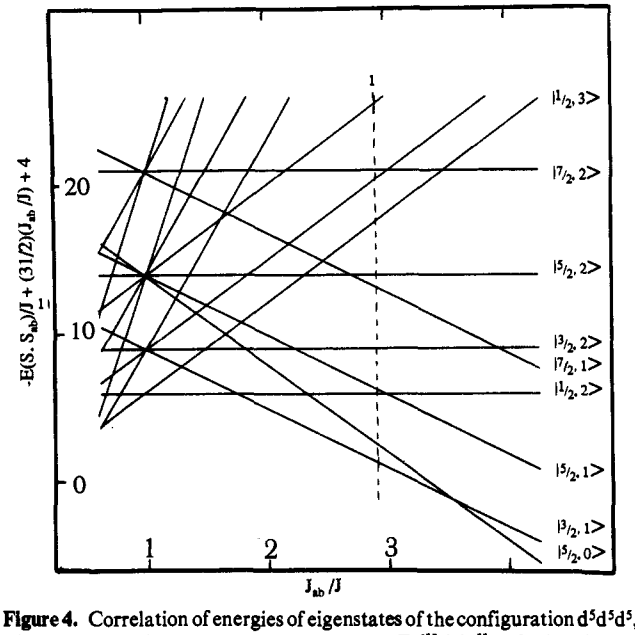

Figure 4. Correlation of energies of eigenstates of the configuration $d^5d^5d^5$, with one nonequivalent atom, e.g. the cluster $Fe^{III}_2Mn^{II}$, calculated from eq 3. The dotted vertical line indicates the value of J_{ab}/J used to fit the spectra reported in this work.

S = 1 has been published on the basis of other data.[12,14,26] With this choice, a least-squares fit of energies gives J_{ab} = −63.5 and J = −28.4 cm^{-1}.

Calculated energies and intensities are listed in Table II. It is of interest that both choices of ground state give hot bands at

(26) Takano, M.; Shinjo, T.; Blake, A. B. *Jpn. J. Appl. Phys.* **1987**, 26 (Suppl. 26-3), 845.
(27) Blake, A. B., private communication.

Table I. Comparison of Predicted and Observed IINS Spectra of $[Fe^{III}_2Mn^{II}O(OOCMe)_6(py)_3](py)$

transition					intensity[b]	energy		assignment
S	S_{ab}	S'	S'_{ab}	energy[a]	I_0	calcd[c]	obsd[d]	band
3/2	1	5/2	0	$-7J + 2J_{ab}$	70/3	24.3	19.4[e]	1
3/2	1	5/2	1	$-5J$	42/5	104.5	102.2	2b
3/2	1	1/2	2	$7J - 4J_{ab}$	64/5	97.7	79.1	2a
3/2	1	3/2	2	$4J - 4J_{ab}$	448/25	160.4	151.7	3
3/2	1	5/2	2	$-J - 4J_{ab}$	896/75	264.9	263.0	4
5/2	0	5/2	1	$2J - 2J_{ab}$	35	80.2	≈80[e]	5*
5/2	0	7/2	1	$-5J - 2J_{ab}$	140/3	226.5	235[e]	6*

[a] Expression derived from eq 3. [b] From eqs 10 and 15. [c] From the expressions listed in column 5, using the parameters J and J_{ab} listed in Table III. [d] Band maxima calculated by Gaussian fitting to the curve, as illustrated in Figure 2, using the same band width for each peak, calculated from the resolution function of the instrument, at the relevant incident beam energy. [e] From spectra at T = 50 K.

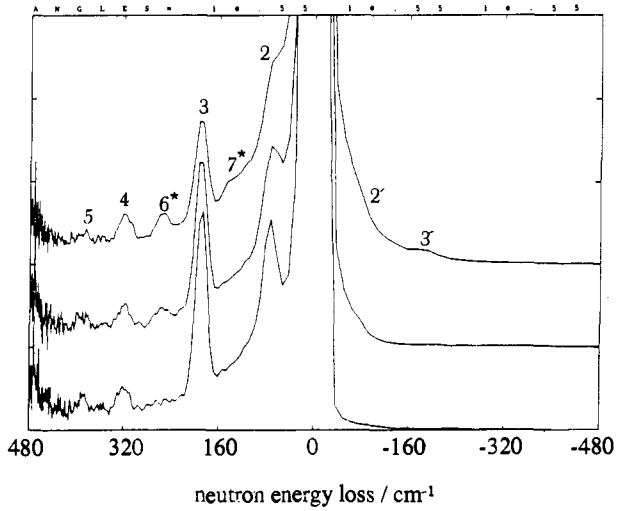

Figure 5. IINS spectra of $[Fe_2NiO(OOCMe)_6(py)_3](py)$. Reading upwards: T = 5, 50, 125 K; the incident neutron beam energy is 68 meV. The average scattering angle (2θ) = 18.6°. Bands marked 2′ and 3′ in the up-scattering ranges are considered to be de-excitations corresponding to bands 2 and 3.

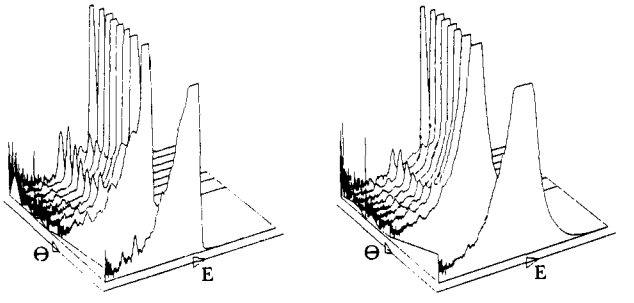

Figure 6. Angular variation of IINS spectra of $[Fe_2NiO(OOCMe)_6(py)_3](py)$. Left: T = 5 K. Right: T = 125 K. Average scattering angles (2θ), reading from the back, are 10.7, 15.8, 20.3, 24.8, 30.8, 37.7, 46.1, 86.5°.

148 and 261 cm^{-1}. A weak, hot, and magnetic band at ca. 255 cm^{-1} has already been noted, and there is at least the possibility of another at *ca.* 144 cm^{-1} in the spectrum at 125 K (Figure 5, band 7*). The intensities of the principal bands observed at 5 K are also reasonably well fitted. Calculated area ratios, bands 1:2:3, are 1:3:7.5; the measured areas are roughly 1:2.9:4.8.

Discussion

The assigned ground states and fitted exchange parameters are summarized in Table III and compared with results from other methods. For the Fe_2Mn complex, Blake and co-workers[14] obtained a good fit to the HDVV model, from magnetic

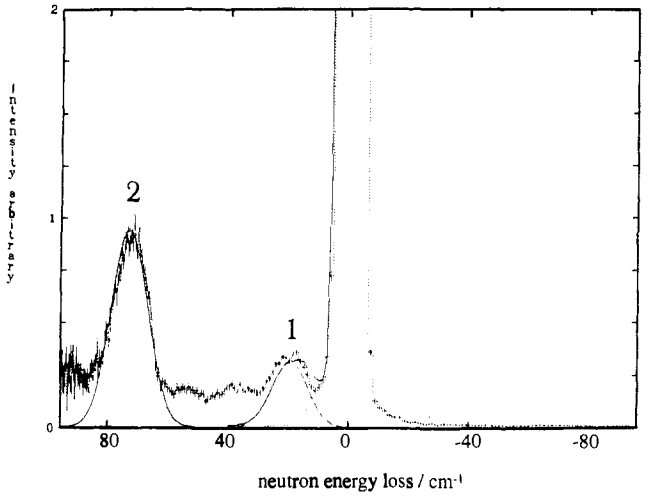

Figure 7. IINS spectrum of $[Fe_2NiO(OOCMe)_6(py)_3](py)$ at $T = 5$ K, with an incident neutron beam energy of 16.7 meV. The average scattering angle (2θ) = 18.6°. Original data points are shown with error bars, and joined by dotted lines. Broken lines indicate Gaussians fitted to the data with a flat linear baseline; full lines are sums of the calculated bands.

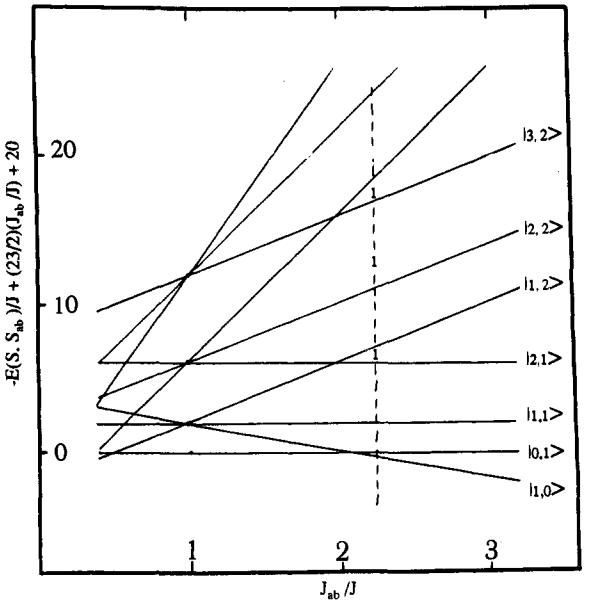

Figure 8. Correlation of energies of eigenstates of the configuration $d^5d^5d^8$, e.g. the cluster $Fe^{III}_2Ni^{II}$, calculated from eq 3. The dotted line indicates the value of J_{ab}/J used to fit the spectra reported in this work.

susceptibility measurements over a wide range of temperatures. Our values of J_{ab} and J agree well with theirs, and we believe they improve the accuracy. The assignment of the ground state with $S = {}^3/_2$ also agrees with the hyperfine Mössbauer measurements of Takano, Shinjo, and Blake.[26] For the Fe_2Ni complex Blake and co-workers[12,14] found $J_{ab} = -73$ and $J = -22$ cm^{-1}. In this case the difference from our data is slightly greater, but the $S = 1$ ground state, deduced from the bulk susceptibility and the hyperfine Mössbauer data,[26] is consistent with the IINS spectra. All authors have assumed molecules of 2-fold symmetry in both compounds, and this is consistent with the limited crystallographic data and with infrared spectroscopy. Crystals of the Fe_2Mn compound are reported to be rhombohedral, space group $P32$, isomorphous with the corresponding mixed-valence complex[15] $[Fe_3O(OOCMe)_6(py)_3](py)$ and with some other mixed-metal complexes.[14] Evidently the Fe_2Mn triangular units are rotationally disordered to give the observed 3-fold symmetry. Crystals

Table II. Comparison of Predicted and Observed IINS Spectra of $[Fe^{III}_2Ni^{II}O(OOCMe)_6(py)_3](py)$

transition					intensity[b]	energy		assignment
S	S_{ab}	S'	S'_{ab}	energy[a]	I_0	calcd[c]	obsd[d]	band
1	0	0	1	$4J - 2J_{ab}$	35/18	17.0	18.5	1
1	0	1	1	$2J - 2J_{ab}$	35/6	73.4	72	2
1	0	2	1	$-2J - 2J_{ab}$	175/12	187.4	188	3
0	1	1	1	$-2J$	16/3	56.8		
0	1	1	2	$-2J - 4J_{ab}$	32/3	204.0		
1	1	2	1	$-4J$	60	113.6		
1	1	1	2	$4J - 4J_{ab}$	128	147.6	≈145[e]	7*
1	1	2	2	$-4J_{ab}$	24	261.2	255[e]	6*

[a-d] See footnotes to Table I. [e] From spectra at $T = 125$ K.

Table III. Calculated and Observed Magnetic Properties of the Complexes $[Fe^{III}_2M^{II}O(OOCMe)_6(py)](py)$

	$M^{II} = Mn^{II}$		$M^{II} = Ni^{II}$	
	this work	lit	this work	lit
ground state total spin, S	3/2	3/2[a,b]	1	1[a,b]
$J(Fe^{III}–Fe^{III})$/cm^{-1}	−61.0	−64[a]	−63.5	−73[a]
$J(Fe^{III}–M^{II})$/cm^{-1}	−20.9	−21[a]	−28.4	−22[a]

[a] References 12 and 14. [b] Reference 26.

of the Fe_2Ni complex are monoclinic, isomorphous with another series of mixed-metal complexes,[14] and although no complete crystal structure is available, there are indications that the environment of the heteroatom differs from those of the two iron atoms to a greater extent than in the rhombohedral series. This is borne out by the infrared spectra. Vibrations with appreciable metal–ligand stretch character, which appear as single bands in spectra of homonuclear complexes of the present type, are split in the mixed-valence and mixed-metal complexes, and among the complexes of valencey type $M^{III}_2M'^{II}$, the splittings are greatest when M′ = Ni;[5] but there are no indications of any structural difference between the two iron atoms.

The agreement in J values between IINS and bulk magnetic susceptibility studies is better for the Fe_2Mn than for the Fe_2Ni complex. Results from susceptibility measurements are averages over temperature whereas those from IINS spectra are precise estimates at a particular temperature, 4.2 K in the present work. The agreement for the Fe_2Mn complex shows that the J values are essentially independent of temperature over the range of the susceptibility measurements, $T = 4.2$ to 295 K.[14] It seems that J values for Fe_2Ni are more temperature dependent. The trigonally symmetric, disordered Fe_2Mn structure is expected to show an isotropic thermal expansion in the plane perpendicular to the the pseudo-3-fold axis, thus tending to preserve the ratio J_{ab}/J, whereas the monoclinic Fe_2Ni complex would expand anisotropically. Further crystallographic studies, at variable temperature, will be needed to clarify this point. Meanwhile, the minor discrepancy just described should not obscure the fact that in these mixed-metal complexes, the agreement between experiment and the basic HDVV spin-coupling model is excellent. A principal cause of this must be the fact that the Fe^{III}, Mn^{II}, and Ni^{II} centers are orbitally nondegenerate. These systems therefore provide a benchmark against which the magnetic behavior of more complicated systems containing centers such as Fe^{II}, Co^{II}, and Cu^{II} can be judged.

Acknowledgment. We acknowledge valuable discussions with Dr. A. B. Blake, Professor P. Day, Dr. A. P. Murani, and Professor A. J. Thomson. We thank Professor G. Davies for the design of the pyridine distillation apparatus and the staff of the ILL for help with the neutron scattering measurements. Financial support was provided by the Science and Engineering Research Council, the British Council, and Solvay Interox R&D.